


Spring 2014

THE DEVELOPMENT OF 6.7% EFFICIENT COPPER ZINC INDIUM SELENIDE DEVICES FROM COPPER ZINC INDIUM SULFIDE NANOCRYSTAL INKS

Brian Kemp Graeser
Purdue University

Follow this and additional works at: https://docs.lib.purdue.edu/open_access_theses

 Part of the [Inorganic Chemistry Commons](#), and the [Nanoscience and Nanotechnology Commons](#)

Recommended Citation

Graeser, Brian Kemp, "THE DEVELOPMENT OF 6.7% EFFICIENT COPPER ZINC INDIUM SELENIDE DEVICES FROM COPPER ZINC INDIUM SULFIDE NANOCRYSTAL INKS" (2014). *Open Access Theses*. 181.
https://docs.lib.purdue.edu/open_access_theses/181

This document has been made available through Purdue e-Pubs, a service of the Purdue University Libraries. Please contact epubs@purdue.edu for additional information.

PURDUE UNIVERSITY
GRADUATE SCHOOL
Thesis/Dissertation Acceptance

This is to certify that the thesis/dissertation prepared

By Brian Kemp Graeser

Entitled

THE DEVELOPMENT OF 6.7% EFFICIENT COPPER ZINC INDIUM SELENIDE DEVICES
FROM COPPER ZINC INDIUM SULFIDE NANOCRYSTAL INKS

For the degree of Master of Science

Is approved by the final examining committee:

Rakesh Agrawal

Yue Wu

Bryan Boudouris

To the best of my knowledge and as understood by the student in the *Thesis/Dissertation Agreement, Publication Delay, and Certification/Disclaimer (Graduate School Form 32)*, this thesis/dissertation adheres to the provisions of Purdue University's "Policy on Integrity in Research" and the use of copyrighted material.

Rakesh Agrawal

Approved by Major Professor(s): _____

Approved by: Michael Harris

05/02/2014

Head of the Department Graduate Program

Date

THE DEVELOPMENT OF 6.7% EFFICIENT COPPER ZINC INDIUM SELENIDE
DEVICES FROM COPPER ZINC INDIUM SULFIDE NANOCRYSTAL INKS

A Thesis

Submitted to the Faculty

of

Purdue University

by

Brian K Graeser

In Partial Fulfillment of the

Requirements for the Degree

of

Master of Science

May 2014

Purdue University

West Lafayette, Indiana

TABLE OF CONTENTS

	Page
LIST OF TABLES	iii
LIST OF FIGURES	iv
ABSTRACT	v
CHAPTER 1. NANOCRYSTAL SYNTHESIS AND DEVICE FABRICATION ...	1
1.1 Introduction.....	1
1.2 Synthesis of the Nanocrystals	3
1.3 Device Processing.....	5
1.4 Electrical Characterization of the Finished Devices	8
1.5 Conclusion.....	10
CHAPTER 2. FUTURE WORK.....	12
2.1 Short Term.....	12
2.2 Long Term	13
BIBLIOGRAPHY.....	15
APPENDICES	
Appendix A Synthesis Method	18
Appendix B Literature Synthesis Data	18

LIST OF TABLES

Table	Page
Table 1-1 Bulk EDS data for the CZIS nanocrystals and the CZISe films	6
Appendix Table	
Table B-1 Cation ratios in the nanocrystals and selenium treated film for the literature synthesis.....	18

LIST OF FIGURES

Figure	Page
Figure 1-1 XRD of the CZIS nanocrystals and CZISE film. CIS,ZnS,CISE,and ZnSe standards have been added as reference.....	4
Figure 1-2 TEM of image of a) the particles made by the literature synthesis b) particles made by our synthesis	4
Figure 1-3 EDS map and line scan of CZISE film this film was prepared the in the same fashion as the completed devices except that none of the window layers have been deposited.....	6
Appendix Figure	
Figure B-1 The XRD of the literature synthesis nanocrystals is on the left and the XRD of the selenium treated film.....	18

ABSTRACT

Graeser, Brian K. M.S., Purdue University, May 2014. The Development of 6.7 % Efficient Copper Zinc Indium Selenide Devices from Copper Zinc Indium Sulfide Nanocrystals. Major Professor: Rakesh Agrawal.

As solar cell absorber materials, alloys of $\text{CuIn}(\text{S,Se})_2$ and $\text{Zn}(\text{S,Se})$ provide an opportunity to reduce the usage of indium along with the ability to tune the band gap. Here we report successful synthesis of alloyed $(\text{CuInS}_2)_{0.5}(\text{ZnS})_{0.5}$ nanocrystals by a method that solely uses oleylamine as the liquid medium for synthesis. The reactive sintering of a thin film of these nanocrystals via selenization at 500 °C results in a uniform composition alloy $(\text{CuIn}(\text{S,Se})_2)_{0.5}(\text{Zn}(\text{S,Se}))_{0.5}$ layer with micron size grains. Due to the large amount of zinc in the film, the sintered grains exhibit the zinc blende structure instead of the usual chalcopyrite structure of $\text{CuIn}(\text{S,Se})_2$ films. The use of the selenide films as a p-type absorber layer has yielded solar cells with total area power conversion efficiencies as high as 6.7% (7.4% based on active area). These preliminary results are encouraging and indicate that with further optimization this class of materials has promise as the absorber layer in solar cells.

CHAPTER 1. NANOCRYSTAL SYNTHESIS AND DEVICE FABRICATION

1.1 Introduction

One application of chalcogenide materials that has received a great deal of attention has been using them to create absorber layers in solar cells. Materials such as $\text{CuIn}_x\text{Ga}_{1-x}\text{Se}_2$ (CIGSe)(Guo, Ford, Agrawal, & Hillhouse, 2013; Todorov, Gunawan, Gokmen, & Mitzi, 2013)(Guo et al., 2013; Todorov & Gunawan, 2012) and CdTe(Gloeckler, Sankin, & Zhao, 2013) have been used for this purpose, and are currently the most efficient thin film technologies. Efforts are being made to reduce the amount of indium used to make the absorber film and to make it earth abundant. $\text{Cu}_2\text{ZnSnSe}_4$ (CZTSe)(Guo et al., 2010; Winkler, Wang, Gunawan, Hovel, & Todorov, 2013) has received a lot of attention and has been proposed as a solution to this problem since it is indium free, but this material has been unable to reach the performance of the best CIGSe devices. One possible explanation for this is the increased complexity of the quaternary kesterite structure of CZTSe as compared to the tertiary chalcopyrite structure of CIGSe.

In this paper we examined the use of an alloy of CuInSe_2 and ZnSe (CZISE) as an absorber material for a solar cell. This alloy can have the binary zinc blende structure depending on the ratio of ZnSe to CuInSe_2 in the final film. The

band gap of this material can also be adjusted by changing the ratio between the CuInSe_2 and the ZnSe . The band gap can be changed from values as low as 1.05 eV (Ping, Guang-Xing, Zhuang-Hao, Xing-Min, & Dong-Ping, 2010) to values as high as 2.67 (Morkoc et al., 1994) eV, allowing for an optimal band gap to be obtained by controlling the composition. A CZISE device will have a reduced material cost when compared to a CIGSe device and an increased performance when compared to a CZTSe device. This material has been successfully used for other semiconductor purposes already, such as quantum dot light emitting diodes (Xiang et al., 2013; J. Zhang, Xie, & Yang, 2011) and as a photocatalyst (W. Zhang & Zhong, 2011).

We have been able to synthesize copper zinc indium sulfide (CZIS) nanocrystals, and have used them to form copper zinc indium selenide (CZISE) films. These films have been further processed into functional solar cells of efficiencies reaching 6.7% based on total area. We have been able to synthesize these films and convert them into full devices using similar methods to those that have been used to create CIGSe (Guo et al., 2013) devices and CZTSe (Guo et al., 2010) devices previously, hopefully allowing for CZISE to become a replacement for both materials. This method involves sintering sulfide (CZIS) nanocrystals in a selenium atmosphere at 500 °C to form a dense selenide film. Nanocrystals were used to avoid using vacuum processing and insure that the films are compositionally uniform at the nanoscale before the selenium treatment.

1.2 Synthesis of the Nanocrystals

From the x-ray diffraction (XRD) pattern it can be seen that our synthesis method produces the desired CZIS nanocrystals. Figure 1 shows the x-ray diffraction (XRD) pattern for nanocrystals from our synthesis. The sample was prepared on a molybdenum substrate, resulting in the two peaks at 40.5° and 73.7° . The peaks for the synthesized nanocrystals fall in between the peak patterns for CuInS (CIS) and ZnS. This would suggest that the lattice spacings for the synthesized nanocrystals fall in between those for CIS and ZnS, and by Vegard's law, indicating that the material produced in this synthesis was an alloy between CIS and ZnS, namely CZIS (Zhong, Feng, Knoll, & Han, 2003). The XRD pattern also indicates a tetrahedral crystal structure. We hypothesize that the structure is zinc blende which has been reported as the most stable structure for the sulfide compound at $210\text{-}250^\circ\text{C}$ and the cation ratios in our particles (Parasyuk & Voronyuk, 2003).

Due to the broad peaks seen in the XRD, we wanted to examine the nanocrystals using transmission electron microscopy (TEM) to look at their uniformity (see figure 2). The nanocrystals from our synthesis have a diameter of 5-20 nm, and are roughly spherical in shape. We also synthesized CZIS nanocrystals by a different method that was heavily based off a published literature method (J. Zhang et al., 2011) in addition to the one that we have developed (details in the supplemental information). The particles from the

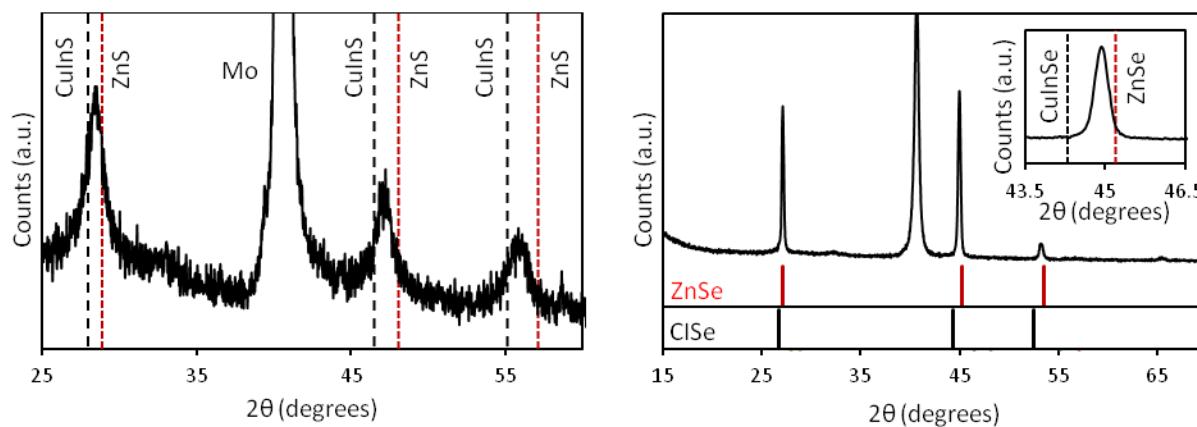


Figure 1-1 XRD of the CZIS nanocrystals and CZISE film. CIS,ZnS,CISE,and ZnSe standards have been added as reference

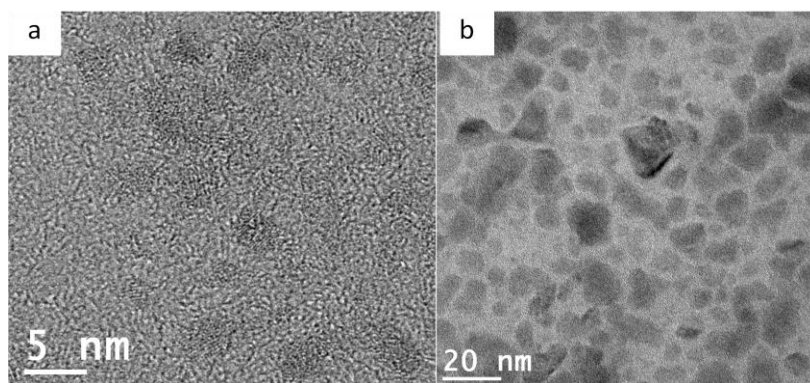


Figure 1-2 TEM of image of a) the particles made by the literature synthesis b) particles made by our synthesis

literature method were smaller and were about 5-10 nm in size. When we examined the XRD of the literature recipe nanocrystals it was inconclusive. We developed our own synthesis method because of the solvents used in each. The motivation for developing our own synthesis method was that the particles produced by the literature synthesis did not disperse well in the solvent used for coating. By changing the synthesis to use a different solvent we were able to achieve much more consistent coatings.

1.3 Device Processing

The XRD pattern changed after the selenium treatment and can be seen in figure #. Since the sample was prepared on molybdenum, there is a signal from molybdenum and from molybdenum selenide and those peaks are marked. The XRD shows the same basic tetrahedral peak pattern as the sulfide nanocrystals, but the pattern is shifted from the nanocrystal pattern due to replacing sulfur with a larger anion, selenium. This causes the lattice to expand and causes a shift in the XRD pattern. The peak locations for our synthesis fall in-between those for CuInSe (CISe) and ZnSe. As with the nanocrystals, this suggests that the film was an alloy of these two materials. The shift might not be complete because not all of the sulfur is replaced by selenium during the treatment. We are confident that this shift is not responsible for the the placement of the peaks inbetween those for CIZSe and ZnSe because a similar shift was seen in the nanocrystals

Table 1-1 Bulk EDS data for the CZIS nanocrystals and the CZISe films

Cation	Fraction of total cations	
	Before Se treatment	After Se treatment
Copper	0.29	0.27
Zinc	0.37	0.35
Indium	0.33	0.38

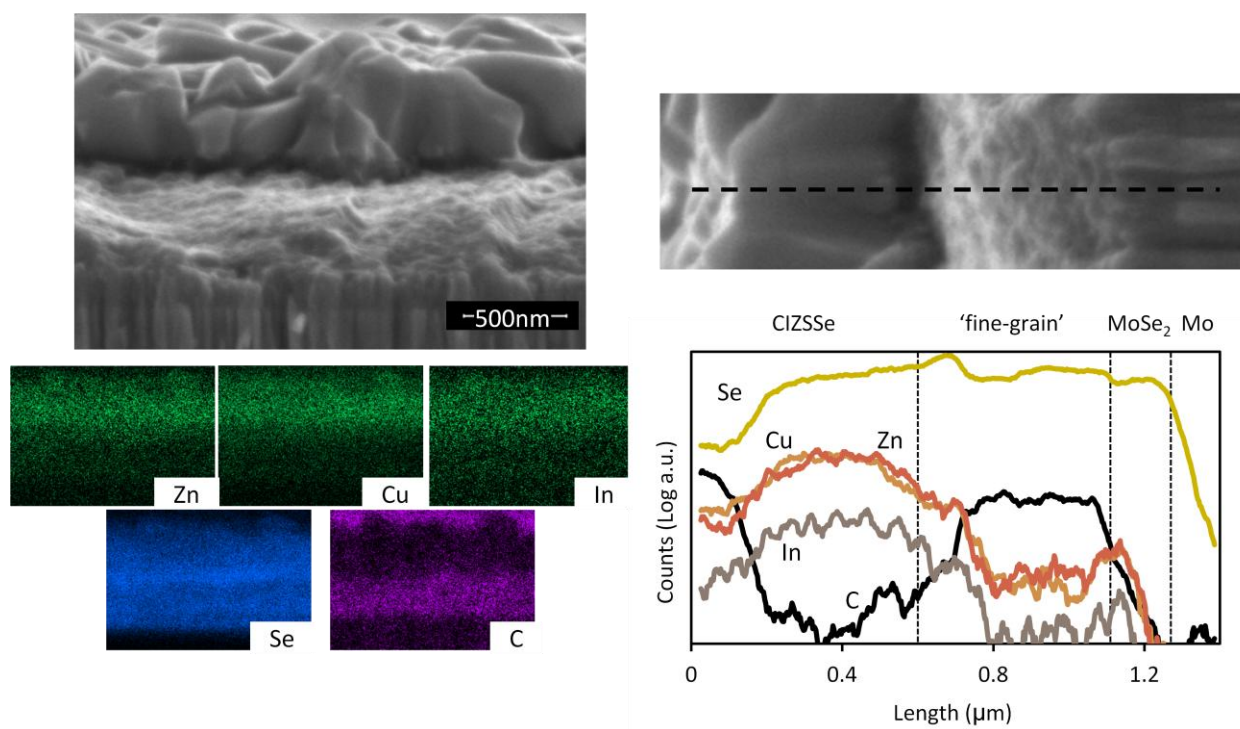


Figure 1-3 EDS map and line scan of CZISe film this film was prepared the in the same fashion as the completed devices except that none of the window layers have been deposited

before the selenium treatment. It can also be observed that the peaks became much sharper after the selenium treatment. This was because of the densification that occurs during the selenium treatment. The film had a cubic zinc blende structure. It is the most thermodynamically favorable structure for CZISE at the cation ratios present in the films (Wagner, Lehmann, Schorr, Spemann, & Doering, 2005). The absence of the tetragonal 101 peak at 17° is further evidence to the cubic structure that we are proposing. This peak is only present in the tetragonal phase and is not present in the cubic.

To confirm the XRD results we looked at the EDS data and the SEM images. These measurements confirmed that the absorber layer in the film was the desired CZISE. In the EDS maps of the film (see figure #) the cations were evenly dispersed throughout the CZISE layer. This shows that the cations were well mixed and that there was no evidence for phase separation in the CZISE layer. There also was no evidence for any sort of composition gradient in the CZISE layer leading us to conclude that this layer was uniform. This was supported by the vertical linescan taken of the film (see figure #). In this there are no visible changes in the cation ratios in the CZISE layer.

In addition to the sintered CZISE layer there was also a 'fine grain' layer beneath it that was observed in the EDS and SEM. This layer was very cation poor and was rich in both carbon and selenium. This layer did not prevent the device from being functional, and it is assumed that this layer was conductive and acted as a continuation of the back contact. This layer has been seen in

similarly processed CIGSe(Guo et al., 2013) and CZTSe(Guo et al., 2010) devices and does not prohibit device performance in those devices either.

1.4 Electrical Characterization of the Finished Devices

In addition to the sintered CZISE layer there was also a 'fine grain' layer beneath it that was observed in the EDS and SEM. This layer was very cation poor and was rich in both carbon and selenium. This layer did not prevent the device from being functional, and it is assumed that this layer was conductive and acted as a continuation of the back contact. This layer has been seen in similarly processed CIGSe(Guo et al., 2013) and CZTSe(Guo et al., 2010) devices and does not prohibit device performance in those devices either.

Devices made from the CZISE films were photoactive and were functional as solar cells. The devices made from our synthesis had a total area efficiency of 6.7%, and 7.4% efficient based off active area. Already in its development, CZISE is only a few percent less efficient than the record liquid processed CZTSSe(Winkler et al., 2013) device, but is still well behind the record for liquid processed CIGSSe(Todorov & Gunawan, 2012). Though when compared to early cells made from these materials(Katagiri et al., 2009; Kazmerski, White, & Morgan, 1976), CZISE performs better and has reached higher efficiencies. This shows great promise for this material, and for it to be able to reach the performance of CIGSe. The J-V curves are shown in figure #. The J_{sc} , V_{oc} and fill factor for these devices were notable, and were comparable to those from quality CZTSSe and CIGSSe devices.

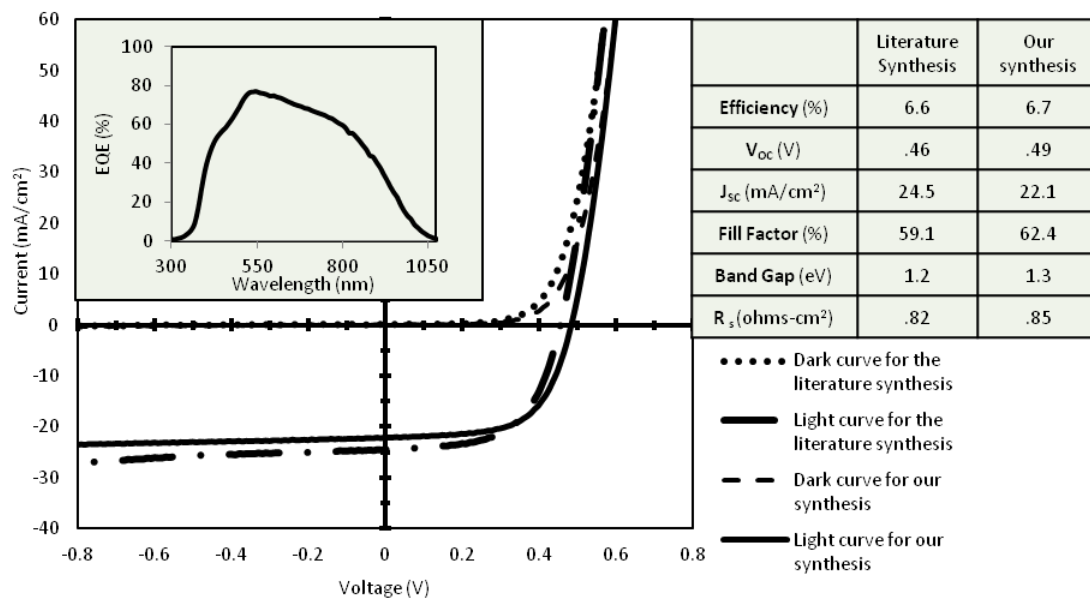


Figure 1-4 J-V characterization for devices made from the literature synthesis and our synthesis. Insert: EQE data for the device made from our synthesis

We wanted to examine the carrier collection in the device using the external quantum efficiency (EQE) (see figure #). We looked at the absorption limited region, the higher wavelengths and found the band gap to be 1.3 eV. The collection for the device was below 80% for all wavelengths. The high slope of the data in the 500-800nm range indicates that there was relatively poor carrier collection through the device. In this region, it was not limited by the absorption, but it instead was limited by the ability of a carrier to get collected (Hegedus & Shafarman, 2004).

We also made a device from particles synthesized by the recipe from literature mentioned earlier (J. Zhang et al., 2011). The device showed a similar champion performance, but was less consistent over the whole coating. Efficiencies varied from 2.0% to 6.6% on the coating that produced the champion efficiency for the literature synthesis, while for our synthesis the efficiencies ranged from 6.0% to 6.7%. Despite the different synthesis techniques that were used to make the nanocrystals, the champion final solar cell performance is the same. It can be seen that they have different V_{oc} and J_{sc} due to differing band gap as a result of varying compositions. Being able to reach notable efficiencies for two different syntheses has shown that this material has the potential to be a viable alternative to CIGSe or CZTSe.

1.5 Conclusion

We have prepared a functional solar cell of greater than 6% efficiency device using CZTSe as the absorber material using liquid based processing. This shows

great promise for this material as a possible replacement for CIGSe in the future. To our knowledge this is the first time a zinc blende CZISe device has been published. We were able to synthesize CZIS nanocrystals by two different syntheses, and found that both of them produce similar results, and both are able to make comparable devices. The two different syntheses did result in slight composition difference that lead to a change in the band gap, and consequently the device parameters.

CHAPTER 2. FUTURE WORK

2.1 Short Term

My plan for the next month is to study and optimize the selenization procedure for my CZIS films. This is a crucial step in the device making process, and is responsible for not only the replacement of sulfur with selenium but it is also responsible for the densification of the film. Optimizing this part of the process has yielded significant improvements in analogous CIGS and CZTS devices. Improving the selenization could lead to improved crystal quality and reduced defects. Reducing the number of defects could lead to less recombination of generated electron-hole pairs in the absorber layer and lead to improved performance. Optimizing selenization can also lead to a reduction in the thickness of the “fine grain” layer. Reducing the thickness of this layer is another way to improve the device. If both of these objectives can be achieved then it could result in a large improvement in the performance of CZISe solar cells. I plan to achieve this by altering certain parameters. I want to examine the effects of time, temperature and box structure. The key variable is what partial pressure is the selenium at during the process and how long does it stay at that pressure before leaving the atmosphere above the CZIS film. I am also planning to look it using a rapid thermal processer (RTP) to have finer control over the

whole process. It may also be possible to look into altering the Se/S ratio in the finished devices to modify the band gap.

2.2 Long Term

The next project that I plan on perusing over the next month is optimizing the cation ratios. I have previously looked into using very high amounts of zinc, a zinc to copper ratio of 9:1. This caused the material to become n-type, and the band gap increased. Changing the amount of zinc can be used to alter the carrier concentration as well as the band gap. My plan is to alter both the amount of zinc and the amount of sulfur in the final film to have two methods of adjusting the band gap. Having the two methods allows me to change the band gap and be selective with the other changes that happen due to changing composition. Controlling the composition may also allow me to control the carrier densities and consequently the width of the space charge region. By increasing the width of the space charge region I can improve carrier collection that is not absorption limited.

As I mentioned in the paragraph above I was able to make n-type CZlSe. My long term plan is to make a homojunction device using this material. By creating this I hope to reduce the amount of interface recombination by removing the interface. I also hope to collect current for the n-type layer. Currently I am using CdS which has too low of carrier lifetime to have the ability to collect carriers. By using a modified version of a functional p-type absorber, I hope to create a function n-type absorber. By using a homojunction I hope to increase

both the J_{sc} and the V_{oc} , and consequently the overall efficiency of a device using CZISE. I plan on doing this by sintering p-type CZISE and n-type CZISE to form a junction. I will have to be able to control the zinc diffusion to preserve the junction, and prevent the whole layer becoming a single uniform composition. I may need to examine multiple methods of depositing and sintering the n-type layer, since the conditions that are right for selenizing, and sintering a standard CZISE device might not be the best conditions for the fabrication of a homojunction. I plan on looking into two step sintering methods. I can selenize the p-type layer the same as a standard heterojunction device. Then I can deposit the n-type layer and perform another sintering step, possibly at a different temperature.

BIBLIOGRAPHY

BIBLIOGRAPHY

- Gloeckler, M., Sankin, I., & Zhao, Z. (2013). CdTe solar cells at the threshold to 20% efficiency. *Photovoltaics, IEEE Journal of*, 3(4), 1389–1393. doi:10.1109/JPHOTOV.2013.2278661
- Guo, Q., Ford, G. M., Agrawal, R., & Hillhouse, H. W. (2013). Ink formulation and low-temperature incorporation of sodium to yield 12% efficient Cu(In,Ga)(S,Se) 2 solar cells from sulfide nanocrystal inks. *Progress in Photovoltaics: Research and Applications*, 21(1), 64–71. doi:10.1002/pip.2200
- Guo, Q., Ford, G. M., Yang, W. C., Walker, B. C., Stach, E. A., Hillhouse, H. W., & Agrawal, R. (2010). Fabrication of 7.2% efficient CZTSSe solar cells using CZTS nanocrystals. *Journal of the American Chemical Society*, 17384–17386. doi:10.1021/ja108427b
- Hegedus, S. S., & Shafarman, W. N. (2004). Thin-film solar cells: device measurements and analysis. *Progress in Photovoltaics: Research and Applications*, 12(23), 155–176. doi:10.1002/pip.518
- Katagiri, H., Jimbo, K., Maw, W. S., Oishi, K., Yamazaki, M., Araki, H., & Takeuchi, A. (2009). Development of CZTS-based thin film solar cells. *Thin Solid Films*, 517(7), 2455–2460. doi:10.1016/j.tsf.2008.11.002
- Kazmerski, L. L., White, F. R., & Morgan, G. K. (1976). Thin-film CuInSe₂/CdS heterojunction solar cells. *Applied Physics Letters*, 29(4), 268. doi:10.1063/1.89041
- , H., Strite, S., Gao, G. B., Lin, M. E., Sverdlov, B., & Burns, M. (1994). Large-band-gap SiC, III-V nitride, and II-VI ZnSe-based semiconductor device technologies. *Journal of Applied Physics*, 76(3), 1363. doi:10.1063/1.358463
- Parasyuk, O., & Voronyuk, S. (2003). Phase diagram of the CuInS₂–ZnS system and some physical properties of solid solutions phases. *Journal of alloys and ...*, 348, 57–64. Retrieved from <http://www.sciencedirect.com/science/article/pii/S0925838802008605>

- Ping, F., Guang-Xing, L., Zhuang-Hao, Z., Xing-Min, C., & Dong-Ping, Z. (2010). Growth and Characterization of CIS Thin Films Prepared by Ion Beam Sputtering Deposition. *Chinese Physics Letters*, 27(4), 046801. doi:10.1088/0256-307X/27/4/046801
- Todorov, T., & Gunawan, O. (2012). Solution processed Cu (In, Ga)(S, Se) 2 absorber yielding a 15.2% efficient solar cell. *Progress in*. doi:10.1002/pip
- Todorov, T., Gunawan, O., Gokmen, T., & Mitzi, D. B. (2013). Solution-processed Cu (In, Ga)(S, Se) 2 absorber yielding a 15.2% efficient solar cell. *Progress in Photovoltaics: Research and Applications*, 21(January 2012), 82–87. doi:10.1002/pip
- Wagner, G., Lehmann, S., Schorr, S., Spemann, D., & Doering, T. (2005). The two-phase region in $2(\text{ZnSe})_x(\text{CuInSe}_2)_{1-x}$ alloys and structural relation between the tetragonal and cubic phases. *Journal of Solid State Chemistry*, 178(12), 3631–3638. doi:10.1016/j.jssc.2005.09.009
- Winkler, M. T., Wang, W., Gunawan, O., Hovel, H. J., & Todorov, T. K. (2013). Optical designs that improve the efficiency of Cu 2 Zn Sn (S,Se) 4 solar cells. *Energy & Environmental Science*, (207890). doi:10.1039/C3EE42541J
- Xiang, W.-D., Yang, H.-L., Liang, X.-J., Zhong, J.-S., Wang, J., Luo, L., & Xie, C.-P. (2013). Direct synthesis of highly luminescent Cu–Zn–In–S quaternary nanocrystals with tunable photoluminescence spectra and decay times. *Journal of Materials Chemistry C*, 1(10), 2014. doi:10.1039/c2tc00493c
- Zhang, J., Xie, R., & Yang, W. (2011). A Simple Route for Highly Luminescent Quaternary Cu-Zn-In-S Nanocrystal Emitters. *Chemistry of Materials*, 23(14), 3357–3361. doi:10.1021/cm201400w
- Zhang, W., & Zhong, X. (2011). Facile synthesis of ZnS-CuInS₂-alloyed nanocrystals for a color-tunable fluorochrome and photocatalyst. *Inorganic chemistry*, 50(9), 4065–72. doi:10.1021/ic102559e
- Zhong, X., Feng, Y., Knoll, W., & Han, M. (2003). Alloyed Zn x Cd_{1-x} S Nanocrystals with Highly Narrow Luminescence Spectral Width. *Journal of the American ...*, 125(44), 13559–63. doi:10.1021/ja036683a

APPENDICES

Appendix A Synthesis Method

For our synthesis we used a modification of the hot injection method. First we prepared a cation precursor solution that consisted of .576 mmol of copper (II) acetylacetonate, .624 mmol of zinc (II) acetylacetonate hydrate, .600 mmol of indium acetylacetonate in 6mL of oleylamine. A sulfur solution was also prepared by putting 1.8 mmol of elemental sulfur in 3 mL of oleylamine. Both solutions were heated up to 60 °C prior to injection. The reaction vessel was charged with 14 mL of oleylamine. It was vacuum purged at reflux (~130 °C) three times and was refilled with argon after every purge. After the third purge/refill cycle the reaction vessel was heated to 250 °C. Once the temperature had stabilized, we injected 4 mL of the cation precursor solution, and 2 mL of the sulfur solution. We let the reaction sit for 15 min. then took the reaction vessel off of the heating source and let it cool to room temperature.

Once the reacted solution was room temperature, it was split into two 30 mL centrifuge tubes. These tubes were filled the rest of the way with isopropanol, and then centrifuged at 140000 RPM. Then the liquid contents of the tube were discarded. The solid is redispersed in 4 mL of hexane, and the rest of the tube is filled with isopropanol, again it is centrifuged at 14000 RPM, and the liquid is discarded. This process is repeated another time, then three more times except that a 70/30 mixture of methanol/isopropanol is used instead of just the isopropanol. After the particles have been washed in this manner they are dried under nitrogen.

Appendix B Literature Synthesis Data

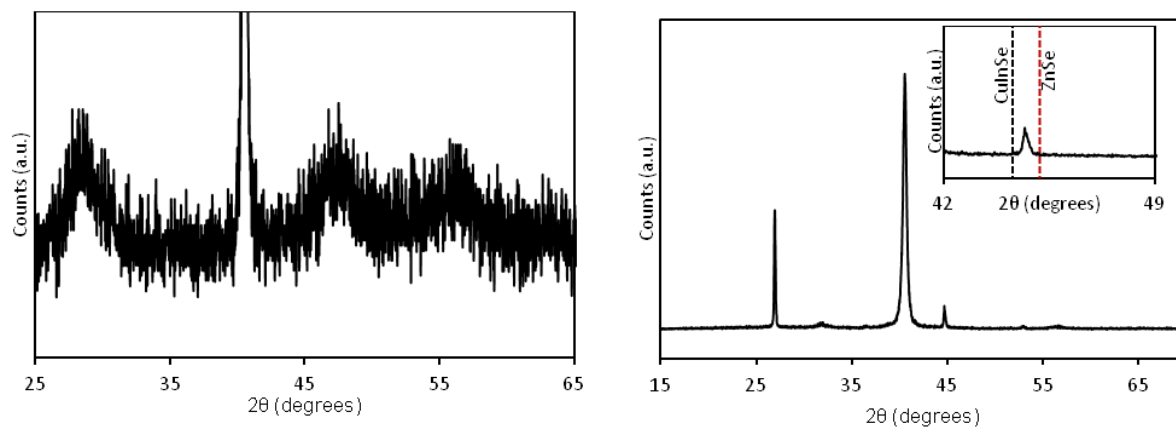


Figure B-4 The XRD of the literature synthesis nanocrystals is on the left and the XRD of the selenium treated film

Table B-2 Cation ratios in the nanocrystals and selenium treated film for the literature synthesis

Cation	Fraction of total cations	
	Before Se treatment	After Se treatment
Copper	0.34	0.29
Zinc	0.40	0.35
Indium	0.26	0.36